



RESEARCH ARTICLE

10.1002/2014PA002669

Key Points:

- Meltwater added to either Labrador Sea or Labrador coast in model experiments
- Ocean and climate responses to coastal forcing too small for 8.2 ka event
- Bias in simulated ocean circulation likely precludes correct outcome

Correspondence to:

C. Morrill,
carrie.morrill@colorado.edu

Citation:

Morrill, C., E. M. Ward, A. J. Wagner, B. L. Otto-Bliesner, and N. Rosenbloom (2014), Large sensitivity to freshwater forcing location in 8.2 ka simulations, *Paleoceanography*, 29, 930–945, doi:10.1002/2014PA002669.

Received 7 MAY 2014

Accepted 12 SEP 2014

Accepted article online 18 SEP 2014

Published online 13 OCT 2014

Large sensitivity to freshwater forcing location in 8.2 ka simulations

Carrie Morrill^{1,2}, Ellen M. Ward³, Amy J. Wagner⁴, Bette L. Otto-Bliesner⁵, and Nan Rosenbloom⁵

¹Cooperative Institute for Research in Environmental Sciences, University of Colorado Boulder, Boulder, Colorado, USA, ²NOAA's National Climatic Data Center, Boulder, Colorado, USA, ³Department of Environmental Earth System Science, Stanford University, Stanford, California, USA, ⁴Geology Department, California State University, Sacramento, Sacramento, California, USA, ⁵Climate and Global Dynamics Division, National Center for Atmospheric Research, Boulder, Colorado, USA

Abstract The 8.2 ka event is a key test case for simulating the coupled climate response to changes in the Atlantic Meridional Overturning Circulation (AMOC). Recent advances in quantifying freshwater fluxes at 8.2 ka from the proxy record have improved the realism of the forcing magnitude in model simulations, yet this forcing is still generally applied in an unrealistic geographic manner, across most of the Labrador Sea rather than just along the Labrador coast. Previous simulations with eddy-resolving ocean models have come to conflicting conclusions regarding the ability of such a coastally confined flow to impact the AMOC. These simulations have also not incorporated full atmosphere models nor have they used the new meltwater forcing values for 8.2 ka. We use the Community Climate System Model, version 3, with an ocean model resolution only slightly coarser than that used in previous eddy-resolving simulations, to test the sensitivity to freshwater forcing location. When revised freshwater forcing is applied across the Labrador Sea, the AMOC is reduced by ~40% and climate anomalies compare well with proxy records of the 8.2 ka event in terms of magnitude and duration. When the forcing is added just along the Labrador coast, however, most meltwater joins the subtropical gyre and travels to the subtropics with minor impact to the AMOC (~10% decrease). It is likely that model biases in the placement of the North Atlantic Current remain an important limitation for correctly simulating the 8.2 ka event.

1. Introduction

The 8.2 ka event has been an important target for model-data comparisons since its hypothesized cause, the catastrophic drainage of proglacial lakes Agassiz and Ojibway into the Hudson Bay, was identified [Barber *et al.*, 1999]. The presumed disruption of the Atlantic Meridional Overturning Circulation (AMOC) at 8.2 ka and its climate impacts could provide an excellent test of the sensitivity of climate models to this sort of buoyancy forcing. Particular features of this event that make it a strong test case are the similar background climate conditions of the early Holocene to today and an event duration and magnitude suitable for model simulations [Schmidt and LeGrande, 2005]. Since the first evidence of meltwater forcing at 8.2 ka emerged, new evidence of AMOC weakening [Ellison *et al.*, 2006; Kleiven *et al.*, 2008] and an abundance of high-resolution, well-dated proxy records of climate change [Morrill *et al.*, 2013a] provide a concrete test of the modeled climate response.

Most previous model experiments of this event were forced by the drainage of proglacial Lake Agassiz-Ojibway into the Hudson Bay and exiting the Hudson Strait. This drainage contained enough water to raise global sea level ~0.2 m or more, but it likely had a short duration on the order of 1 year, though it might have occurred in two separate short-lived pulses [Clarke *et al.*, 2004; Tornqvist and Hijma, 2012]. These past experiments found some success in reproducing the patterns of climate response, which include cooling over the circum-North Atlantic and a southward shift of the Intertropical Convergence Zone [LeGrande and Schmidt, 2008; Tindall and Valdes, 2011; Wiersma *et al.*, 2006]. In general, however, the duration of the modeled event was many decades shorter than the ~150 years indicated by the proxy records [Morrill *et al.*, 2013a], and the magnitude of the anomalies was substantially smaller (e.g., temperature anomalies about half what the proxy record indicated for Europe) [Clarke *et al.*, 2009; Morrill *et al.*, 2013b; Tindall and Valdes, 2011].

Recent advances in quantifying the meltwater forcing associated with the 8.2 ka event point toward a forcing larger than the drainage of Lake Agassiz-Ojibway, however. Work in the Mississippi River Delta and in the Netherlands indicates a much larger sea level rise, on the order of 1.5 to 3.0 m, that occurred very abruptly

around 8.2 ka [Hijma and Cohen, 2010; Kendall et al., 2008; Li et al., 2012]. Geochemical proxies from the Hudson Strait likewise identify a period of elevated meltwater flux associated with the 8.2 ka event that would have exceeded the drainage of Lake Agassiz-Ojibway alone [Carlson et al., 2009]. One likely source for the larger meltwater flux is the disintegration of the Hudson Bay ice dome [Gregoire et al., 2012]. Using the most recent estimates of total meltwater flux around 8.2 ka, Wagner et al. [2013] found a much better match to the proxy record in terms of event duration and magnitude.

An important remaining criticism of 8.2 ka model experiments concerns the way in which meltwater forcing is applied to the ocean models. In some experiments, meltwater is added to a large area of the North Atlantic, e.g., over the entire Labrador Sea [Wagner et al., 2013]. This method of adding freshwater conflicts with physical oceanographic evidence that meltwater exiting the Hudson Strait should be trapped along the coastline of the western Labrador Sea [Wunsch, 2010]. The difference between these two scenarios is significant because meltwater spread over the entire Labrador Sea is sure to impact convection and the rate of deepwater formation, while the same might not be true for a coastally confined flow. Some previous model simulations apply meltwater to an appropriately constrained area of the Hudson Strait or the eastern coast of North America but do not necessarily have the ocean model resolution to simulate a coastally confined flow [LeGrande and Schmidt, 2008; Li et al., 2009; Wiersma et al., 2006].

High-resolution (eddy-resolving) ocean model simulations have further tested sensitivity to meltwater forcing location but have come to conflicting conclusions. Using the UVic Earth System Climate Model, Spence et al. [2008] found little difference in the ocean response to forcing location, but results from the MITgcm ocean model indicate that a coastally confined flow is incapable of producing an 8.2 ka event [Condrón and Winsor, 2011]. Neither of these models was coupled to a full atmosphere model, which could be important for ocean-atmosphere interactions, as well as for assessing the full climate response to the meltwater forcing. In addition, the latter simulation has been criticized for being only a decade long and therefore not precluding a longer-term response to the meltwater forcing [Hoffman et al., 2012]. In addition, only the smaller Lake Agassiz-Ojibway forcing was used in these experiments.

In this study, we use simulations completed with the Community Climate System Model version 3 (CCSM3) to test the climate response to the location of meltwater forcing. Our previous work with this model indicates that it can skillfully simulate the 8.2 ka event when the revised estimate of total meltwater input is applied over the entire Labrador Sea [Morrill et al., 2013b; Wagner et al., 2013]; the goal of this study is to determine if the same holds true when the forcing is applied in a more physically realistic way along the Labrador coast. The simulations completed for this study also address criticisms of previous coastal forcing experiments, namely, that they have used ocean-only models and/or outdated meltwater forcing estimates. The CCSM3 is a fully coupled climate system model with high-resolution atmosphere and ocean component models. While the resolution of the ocean model, which is up to $\sim 0.3^\circ$ latitude in the North Atlantic, is not quite eddy permitting, it is sufficient to maintain a coastally confined flow. We also consider both the smaller Lake Agassiz-Ojibway meltwater input and the larger meltwater input that has been recently inferred from sea level data.

2. Methods

We completed a control simulation and four freshwater forcing experiments using the Community Climate System Model, version 3 (CCSM3) [Collins et al., 2006]. CCSM3 is a global ocean-atmosphere-sea ice-land surface climate model coupled without flux corrections. The atmospheric component is the Community Atmosphere Model version 3 (CAM3) at a horizontal resolution of T42 (an equivalent grid spacing of approximately 2.8° in latitude and longitude) and 26 hybrid vertical levels. The land model, which includes river routing and prescribed plant functional types, uses the same grid as the atmospheric component. The ocean model is a version of the Parallel Ocean Program model with a nominal grid spacing of approximately 1° in latitude and longitude and greater resolution in the tropics and North Atlantic (approximately 0.3° in latitude). The vertical resolution is 40 levels extending to a depth of 5.5 km. The dynamic-thermodynamic sea ice model uses the same horizontal grid and land mask as the ocean component.

Given the importance of a realistic model representation of the North Atlantic for this research, we review briefly here the relevant features of the CCSM3 in relation to modern observations. A detailed comparison of ocean model properties with observations is presented in Large and Danabasoglu [2006]. They find realistic transports in the subtropical and subpolar gyres in the North Atlantic, but a modeled North Atlantic

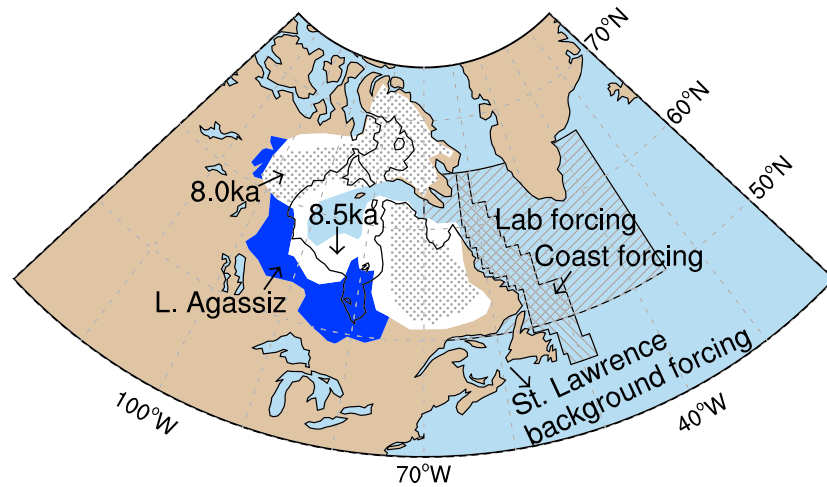


Figure 1. Area of Lake Agassiz-Ojibway at 8.5 ka (blue) and the Laurentide Ice Sheet at 8.5 ka (white) and 8.0 ka (stippling). Also shown are the locations of freshwater forcing applied in the CCSM3 experiments, including the early Holocene background meltwater flux added to the St. Lawrence River and the 8.2 ka event forcing applied to either the Labrador Sea (Lab) or the Labrador coast (Coast). Lake and ice sheet areas are from Dyke [2004].

Current that is too wide and too zonal, which leads to some sea surface temperature and salinity biases. Deficiencies in simulating western boundary currents are very common in models of this resolution. Despite these biases, the maximum AMOC stream function, excluding the shallow wind-driven overturning, in a preindustrial control simulation of the CCSM3 is 19.1 ± 1.0 sverdrup (Sv) [Otto-Bliesner *et al.*, 2006], within the error of the present-day observations of 16 ± 2 Sv and 18 ± 2.5 Sv [Ganachaud, 2003; Lumpkin and Speer, 2007]. In addition, the CCSM3 does well in simulating perturbations to the AMOC under past climate states such as the Last Glacial Maximum when compared against relevant proxy data [Otto-Bliesner *et al.*, 2007].

We first completed a control simulation (CTL) with boundary conditions appropriate for 8.5 ka. This simulation is the same as the CTL-ALL simulation described in Wagner *et al.* [2013]. Atmospheric greenhouse gas concentrations were set to early Holocene values derived from Antarctic ice cores [Flückiger *et al.*, 2004; Monnin *et al.*, 2001], with $\text{CO}_2 = 260$ ppm, $\text{CH}_4 = 660$ ppb, and $\text{N}_2\text{O} = 260$ ppb. Orbital parameters were prescribed from the astronomical calculations of Berger [1978] for 8.5 ka (eccentricity = 0.019199, obliquity = 24.22° , longitude of perihelion = 319.50°), which yield greater insolation in the Northern Hemisphere during boreal summer and lower insolation during boreal fall and winter compared to present day. At 60°N , for example, maximum and minimum monthly insolation anomalies are in June ($+37 \text{ W/m}^2$, +8%) and October (-25 W/m^2 , -18%), respectively, at 8.5 ka compared to 0 ka. The remnant Laurentide Ice Sheet located around Hudson Bay was defined from ICE-5G (Figure 1) [Peltier, 2004]. Prior to the final drainage of Lake Agassiz and collapse of the Laurentide Ice Sheet (LIS), there was a small baseline flow of glacial runoff down the St. Lawrence River. Based on numerical reconstructions of the LIS during deglaciation, the flow was estimated by Licciardi *et al.* [1999] to have been 0.05 Sv. We prescribe this baseline flow as runoff to the ocean at the mouth of the St. Lawrence River. Previous experiments we completed of the 8.2 ka event both with and without this baseline flow yield very similar results, suggesting that the baseline flow does not have a large impact on our conclusions [Wagner *et al.*, 2013]. The CTL simulation was branched from an equilibrium simulation for 8.5 ka with all the above boundary conditions minus the baseline flow of glacial runoff down the St. Lawrence River. The CTL simulation was integrated with the 8.5 ka boundary conditions including the baseline flow for over 400 years until surface salinity stabilized. Global mean ocean salinity decreases slowly through the CTL simulation due to the background meltwater flux, a trend that parallels observed freshening during the late glacial and early Holocene. It is conceivable that this salinity trend could influence the transient behavior of the ocean to freshwater perturbations, both in nature and in models, and this should be the subject of future work.

These boundary conditions yield a realistic representation of the early Holocene in the CCSM3 when compared to proxy data for sea surface temperature, sea surface salinity, AMOC strength, and mixed layer depth. A detailed proxy comparison has been presented in Wagner *et al.* [2013] and is briefly summarized here. For

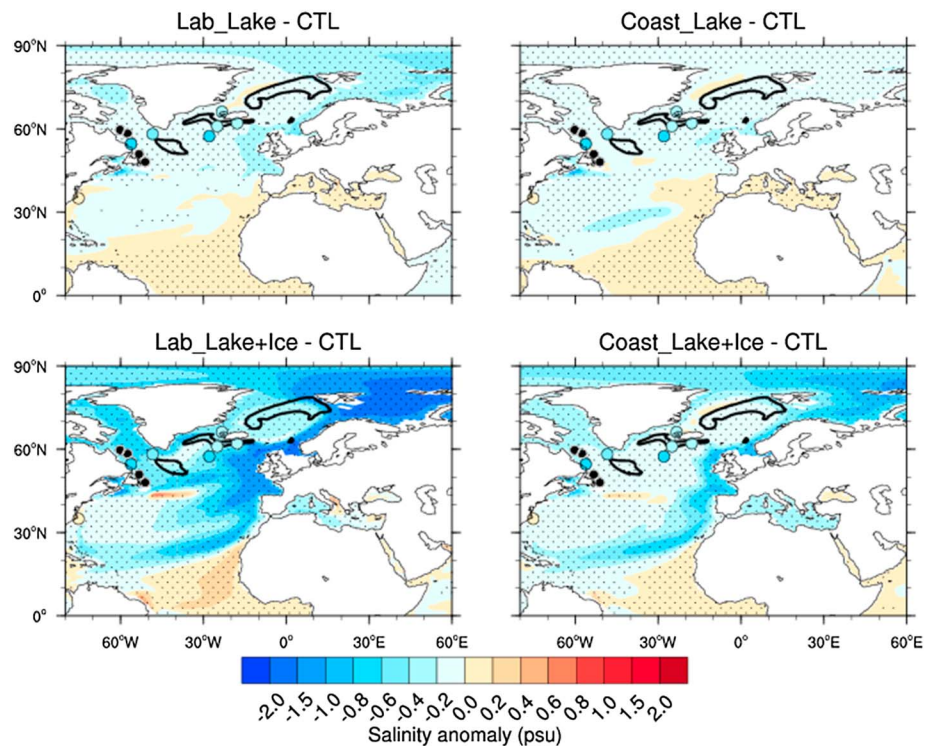


Figure 2. Annual salinity anomalies at 100 m depth for the four experiments relative to the control (CTL) simulation, in practical salinity units. Anomalies have been calculated over the entire period of meltwater forcing and recovery, 50 years for the Lake experiments and 150 years for the Lake + Ice experiments. Stippling indicates anomalies that are statistically significant at the 95% level according to a Student's *t* test. Convection areas, defined as having annual mixed layer depth greater than 200 m, are outlined in black. Locations of cores HU87033-017 (54.6°N, 56.2°W) [Hoffman *et al.*, 2012], MD99-2227 (58.2°N, 48.4°W) [Winsor *et al.*, 2012], MD99-2251 (57.4°N, 27.9°W) [Ellison *et al.*, 2006], Rapid-12-1 k (62.1°N, 17.8°W) [Thornalley *et al.*, 2009], ODP 984 (61°N, 25°W) [Came *et al.*, 2007], MD99-2266 (66.2°N, 23.3°W) [Quillmann *et al.*, 2012], and MD99-2203 (35.0°N, 75.2°W) [Cléroux *et al.*, 2012] with $\delta^{18}\text{O}_{\text{seawater}}$ measurements of the 8.2 ka event are indicated by circles colored to correspond to practical salinity unit values from the model color bar. Values of $\delta^{18}\text{O}_{\text{seawater}}$ were converted to practical salinity units by assuming the oxygen isotopic composition of Laurentide Ice Sheet meltwater was -25‰ [Hillaire-Marcel *et al.*, 2007]. Locations of cores that contain detrital carbonate associated with the 8.2 ka event [Lewis *et al.*, 2012] are shown by black dots.

example, the proxy-inferred warming in the East Greenland Current [Andersen *et al.*, 2004a, 2004b] and cooling in the Irminger Basin [Ellison *et al.*, 2006; Farmer *et al.*, 2008; Thornalley *et al.*, 2009] during the early Holocene as compared to the preindustrial period are both reproduced by the model. The simulations also show the relatively fresher conditions across the North Atlantic as recorded by early Holocene proxies [deVernal and Hillaire-Marcel, 2006; Solignac *et al.*, 2006; Thornalley *et al.*, 2009]. The simulated strength of the AMOC in our early Holocene CTL simulation is 16.7 ± 1.1 Sv, slightly weaker than the preindustrial control value of 19.1 ± 0.9 Sv. This result is consistent with proxies, which show small to no change in AMOC strength between the early and late Holocene [Hall *et al.*, 2004; McManus *et al.*, 2004; Oppo *et al.*, 2003; Praetorius *et al.*, 2008]. Lastly, convection areas simulated for the early Holocene exist in the Greenland-Iceland-Norwegian (GIN) Seas, the Irminger Basin, and east of the Labrador Sea (Figure 2). These locations do not contradict proxy evidence for decreased convection in the Labrador Sea proper and strong convection in the Irminger Basin and/or GIN Seas in the early Holocene compared to present [Hall *et al.*, 2010; Hillaire-Marcel *et al.*, 2001].

Four experiments test the importance of meltwater forcing volume and location (Table 1). All experiments are initially forced with a flux and duration of meltwater of 2.5 Sv for 1 year, (volume of $0.79 \times 10^4 \text{ m}^3$ or 0.2 m of sea level rise), which represents the best estimate from hydraulic modeling for the drainage of Lake Agassiz-Ojibway [Clarke *et al.*, 2004]. Experiments termed "Lake + Ice" then receive an additional meltwater forcing of 0.13 Sv for 99 years (total volume of $4.85 \times 10^4 \text{ m}^3$ or 1.35 m of sea level rise), which represents the contribution of the Hudson Bay ice dome. The ice dome forcing is calculated by combining estimates of

Table 1. Meltwater Experiments Defined by Name and Forcing

Forcing Location	Forcing Magnitude and Duration	
	Labrador Sea (50°–65°N, 35°–70°W) Labrador Coast (Figure 1)	2.5 Sv for 1 year Lab_Lake Coast_Lake

freshwater discharge through the Hudson Strait during the 8.2 ka event that were inferred from the U/Ca of sediment cores to be 0.13 ± 0.3 Sv [Carlson *et al.*, 2009] with a total volume of freshwater release estimated to be 1.5 ± 0.7 m based on measured sea level rise [Li *et al.*, 2012]. A sensitivity study presented in Wagner *et al.* [2013] shows that compressing the same volume of ice dome forcing into five rather than 99 years does not affect our results. The sensitivity of our results to changes in the volume of freshwater forcing or to lengthening the forcing period is unknown, however. The location of meltwater forcing in our experiments is set to either the Labrador Sea (50°–65°N, 35°–70°W) or to an area of 302 grid cells along the west coast of the Labrador Sea, as shown in Figure 1. Applying the “Coast” freshwater forcing to a more restricted area in the Hudson Bay or Hudson Strait was not feasible because our ocean model has a fixed volume. In such a model, freshwater is applied as a virtual salinity flux and sea surface salinity can become negative if too much freshwater is added to a very small area. Thus, we chose the location and number of grid cells in the Coast experiments to best reflect the theoretical pathway of water leaving the Hudson Strait. The two “Lab” experiments, called “Lab_Lake” and “Lab_Lake + Ice” in this paper, were previously presented in Wagner *et al.* [2013] as Lake_weak and Lake + Ice_100 years, respectively, while the two Coast experiments are presented here for the first time. Following the end of the meltwater forcing period, all simulations were integrated at least another 50 years to capture the recovery period.

3. Results

3.1. Upper Ocean Salinity

There are significant differences between the Lab and Coast experiments in the path of meltwater transport in the North Atlantic, as shown by near-surface salinity anomalies and the zonal average cross section of Atlantic salinity (Figures 2 and 3). In Figure 2, we plot salinity at 100 m depth as the model level most similar to the depth habitat of the forams used in salinity reconstructions [Came *et al.*, 2007; Hoffman *et al.*, 2012;

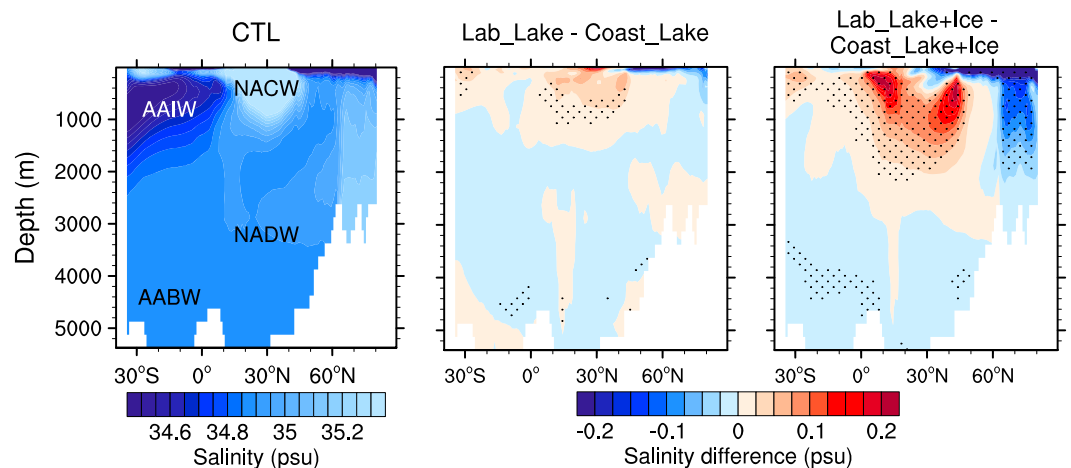


Figure 3. Zonal average cross sections of Atlantic Ocean salinity in the (left) control simulation and (middle, right) salinity difference between meltwater experiments, in practical salinity units. In the control plot, abbreviations show the approximate locations of Atlantic water masses as indicated by salinity values: AAIW = Antarctic Intermediate Water, AABW = Antarctic Bottom Water, NACW = North Atlantic Central Water, and NADW = North Atlantic Deep Water. Differences have been calculated over the entire period of meltwater forcing and recovery, 50 years for the Lake experiments and 150 years for the Lake + Ice experiments. Stippling indicates differences that are statistically significant at the 95% level according to a Student’s *t* test. In the difference plots, red colors show areas that are fresher in the Coast relative to the Lab experiments and blue colors show areas that are fresher in the Lab relative to the Coast experiments.

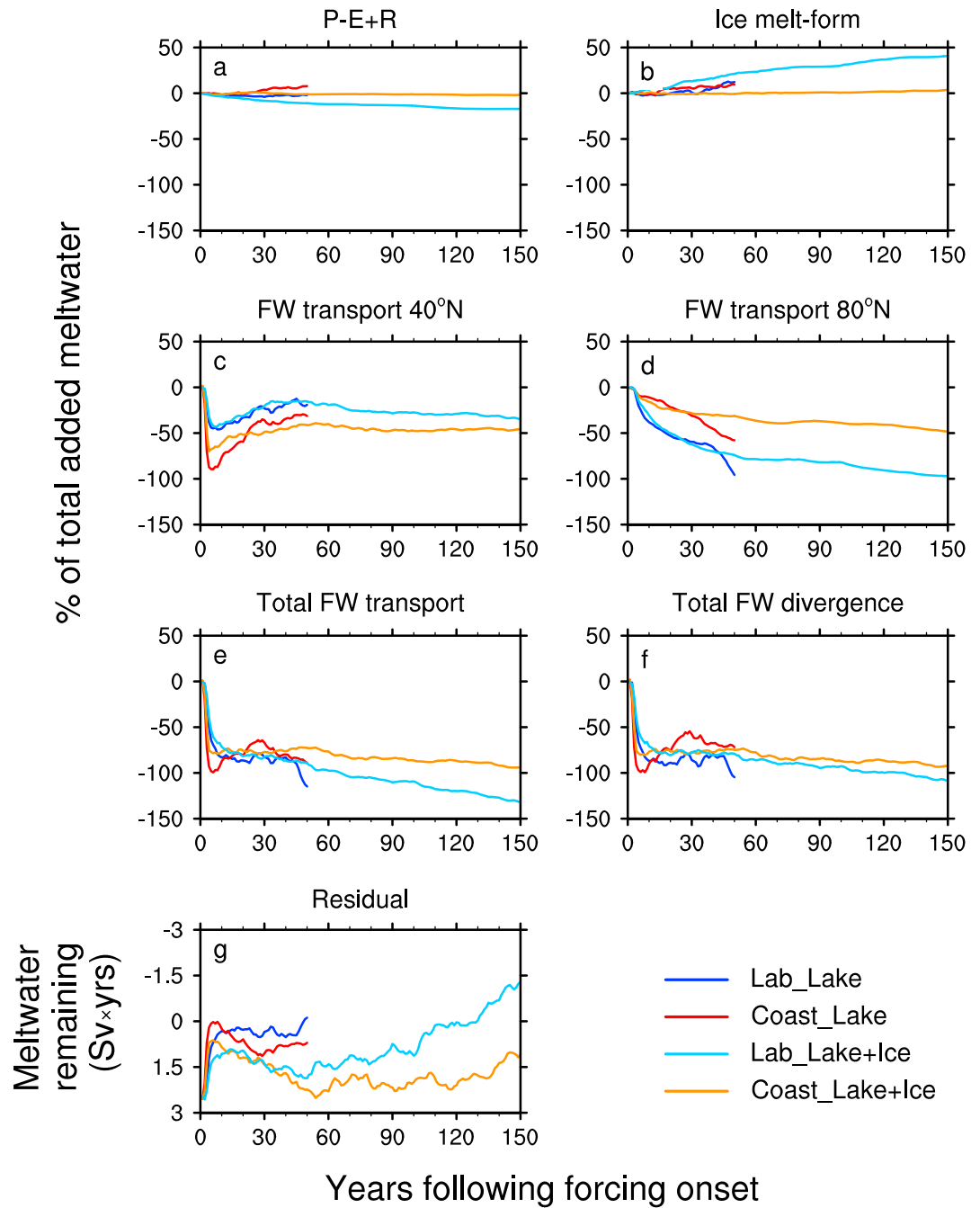


Figure 4. Freshwater balance in the North Atlantic (40°–80°N), calculated as cumulative anomalies from control simulation and expressed relative to total amount of meltwater added in each experiment: (a) surface freshwater input from precipitation minus evaporation plus runoff, (b) surface freshwater input from sea ice melt minus formation, (c) freshwater transport across 40°N, (d) freshwater transport across 80°N, (e) total freshwater transport (sum of Figures 4c and 4d) out of the 40°–80°N region, (f) total freshwater divergence (sum of Figures 4a–4d) out of the region, and (g) residual amount of freshwater remaining in the region. Positive (negative) numbers indicate a freshwater gain to (loss from) the 40°–80°N region. The latitude of 80°N is defined as along the line of 80°N latitude from 90°W to 30°E and along the line of 30°E from 80° to 70°N.

Quillmann et al., 2012; Thornalley et al., 2009; Winsor et al., 2012]. In both Lab and Coast cases meltwater is transported eastward in the North Atlantic Current at about 45°N, thereafter continuing northeastward into the Greenland-Iceland-Norwegian (GIN) Seas and southwestward in the subtropical gyre. The GIN Seas become fresher in the Lab compared to the Coast experiments (Figures 2 and 3). There is also more meltwater

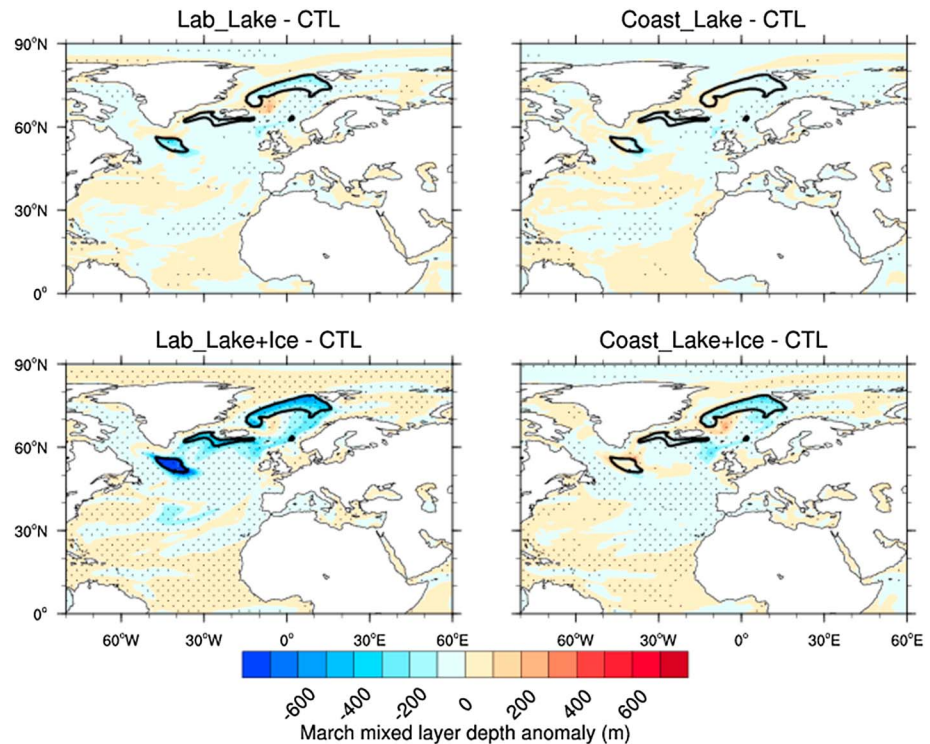


Figure 5. March mixed layer depth anomalies for the four experiments relative to the control (CTL) simulation, in meters. Anomalies have been calculated over the entire period of meltwater forcing and recovery, 50 years for the Lake experiments and 150 years for the Lake + Ice experiments. Stippling indicates anomalies that are statistically significant at the 95% level according to a Student's *t* test. Control simulation convection areas, defined as having annual mixed layer depth greater than 200 m, are outlined in black.

entrainment into the subpolar gyre in the Lab experiments, not surprising given that meltwater forcing is overlain on the gyre in these experiments. The Coast experiments, on the other hand, show greater freshening south of 45°N at depths between 200–1000 m and 200–2000 m in the Lake and Lake + Ice experiments, respectively (Figure 3).

The difference in the spatial distribution of meltwater is corroborated by the total vertically integrated freshwater budget of the North Atlantic (Figure 4). Time series in Figures 4 a–4d separate components of the freshwater budget, showing the extent to which each of these components adds (positive values) or removes (negative values) freshwater from the North Atlantic. Values plotted on the y axis are expressed cumulatively relative to the total amount of meltwater added in the simulation; for example, a value of –100% indicates complete divergence from the North Atlantic of all meltwater that had been added up until that point in time. The total atmospheric freshwater flux anomaly relative to the control simulation is minor in all cases (Figure 4a). The same is true for the sea ice freshwater flux in all cases except Lab_Lake + Ice, in which an increased influx and melting of Arctic sea ice freshens the North Atlantic relative to the control simulation (Figure 4b). The Coast experiments have greater southward freshwater transport at 40°N than their corresponding Lab experiment; the opposite is true for northward freshwater transport at 80°N (Figures 4c and 4d). The combined northward and southward freshwater transport out of the North Atlantic is greater in the Lab_Lake + Ice than in the Coast_Lake + Ice experiment (Figure 4e), but this difference becomes negligible when accounting for freshwater exported north to the Arctic Ocean in the Lab_Lake + Ice experiment that returns southward in the form of sea ice and melts (Figures 4b and 4f). Regardless of the directionality of freshwater transport, the vast majority of meltwater input has been diverted from the North Atlantic deepwater formation areas, which are located between 40°N and 80°N, by the end of all four simulations (i.e., complete divergence equals values of –100% in Figure 3f and 0 Sv × years in Figure 4g). This signifies significant progress toward recovery of North Atlantic salinity within 50 years following the end of meltwater input. Small trends still exist at the end of all four experiments as the North Atlantic continues to

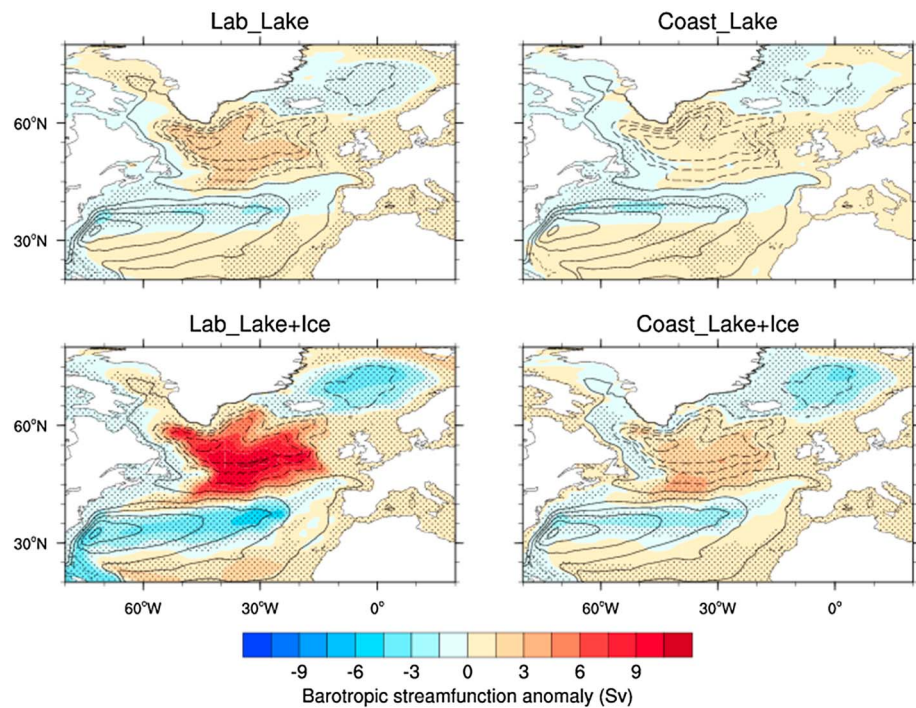


Figure 6. Control values for barotropic stream function (contour lines) and stream function anomalies calculated over the entire period of meltwater forcing and recovery, 50 years for the Lake experiments and 150 years for the Lake + Ice experiments, in Sv (colored contours). The contour interval for the control values is 10 Sv. Dashed lines show negative stream function values or a cyclonic circulation. Positive (negative) anomalies for a cyclonic (anticyclonic) circulation indicate weakening of the circulation. Stippling shows statistical significance for anomalies at the 95% level according to a Student's *t* test.

become saltier. While we cannot rule out the possibility of additional meltwater-induced climate and ocean change after the end of our experiments, we think this is unlikely for two reasons. First, longer deglacial experiments completed with a low-resolution version of the CCSM3 show a linear recovery of the AMOC once meltwater forcing stops, with no hysteresis or multiple equilibria [Liu *et al.*, 2009]. Second, the ocean model efficiently mixes meltwater both vertically (Figure 3) and horizontally (Figure 4), leading to diffuse freshwater anomalies by the end of our experiments that do not have the same intensity that the original forcing did.

The Lab_Lake + Ice experiment shows the best agreement between quantitative proxy reconstructions of salinity and modeled salinity at 100 m water depth according to the root-mean-square error (Figure 2, root-mean-square error of 0.06 practical salinity unit (psu) for Lab_Lake + Ice compared to values between 0.14 and 0.16 psu for the other three experiments). Salinity anomalies across the subpolar North Atlantic in the other three experiments are much smaller than in Lab_Lake + Ice, leading to greater model-data disagreement. This result holds true even after correcting for the fact that the Lake experiments are only 50 years in duration and show nearly complete recovery of sea surface salinity at that time, while the anomalies in the Lake + Ice experiments are similar in duration to those recorded in proxies, on the order of 150 years long [Morrill *et al.*, 2013a]. It appears that the meltwater volume is too small in the Lake-only experiments and also that correct simulation of salinity anomalies with the larger Lake + Ice forcing requires more entrainment of meltwater into the subpolar gyre and less southward transport into the subtropical gyre than is present in the Coast experiments.

3.2. Atlantic Meridional Overturning Circulation

Increased northward transport of meltwater to the GIN Seas as well as increased entrainment in the subpolar gyre in the Lab experiments compared to the Coast experiments leads to greater impacts on surface buoyancy in North Atlantic convection areas and on deepwater formation. The location of the main convection areas in the CCSM3 is shown in Figure 2; these include the east Labrador Sea, Irminger-Iceland Basins, and GIN Seas. These locations are not inconsistent with early Holocene proxy records, given the

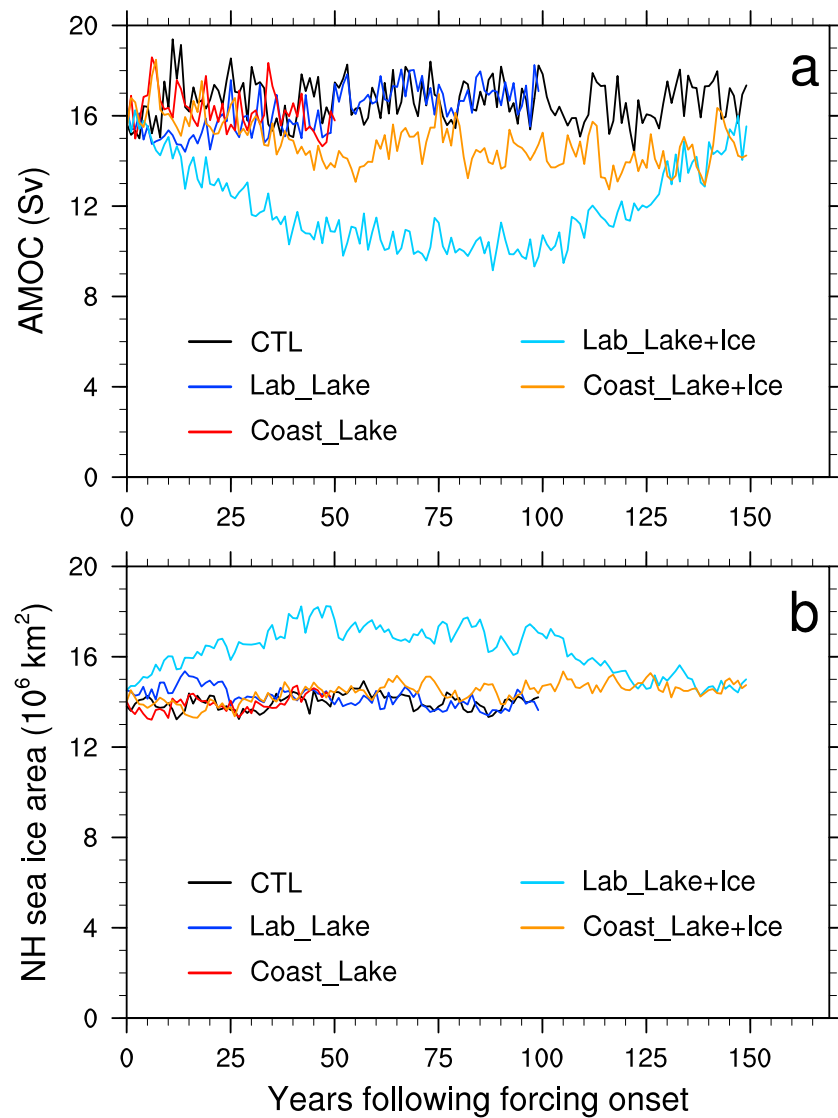


Figure 7. (a) Atlantic meridional overturning circulation time series, in sverdrups ($1 \text{ Sv} = 10^6 \text{ m}^3/\text{s}$) and (b) Northern Hemisphere annual sea ice area time series, in 10^6 km^2 , for the control simulation and the four experiments. AMOC is defined as the maximum of the Atlantic overturning stream function excluding the surface ($<500 \text{ m}$) wind-driven overturning circulation.

difficulties and uncertainties in reconstructing convection [Wagner *et al.*, 2013]. Some micropaleontological evidence published by Hillaire-Marcel *et al.* [2001] suggests that convection began only after $\sim 8 \text{ ka}$ at core sites west of our modeled Labrador Sea convection area; additional proxy records are needed to determine whether this result applies across the entire Labrador Sea region. Reduction of mixed layer depth following meltwater forcing is greater in the Lake + Ice experiments than in their corresponding Lake experiments and greater in the Lab experiments than in their corresponding Coast experiments (Figure 5). Likewise, the North Atlantic subpolar gyre circulation shows a greater reduction in strength in the Lab experiments than in their corresponding Coast experiments, consistent with the greater buoyancy forcing that occurs in the Labrador Sea in the Lab experiments (Figure 6).

Not surprisingly, experiments with greater reductions in mixed layer depth show greater reductions in the strength of the AMOC. The greatest AMOC weakening ($\sim 40\%$) occurs in the Lab_Lake + Ice experiment, while the maximum decrease in AMOC is much smaller ($\sim 15\%$) in the Coast_Lake + Ice experiment and smaller yet in the two Lake experiments ($< 10\%$; Figure 7a). The duration of AMOC reduction is closely linked to the duration of meltwater forcing, with recovery generally beginning soon after the cessation of the forcing.

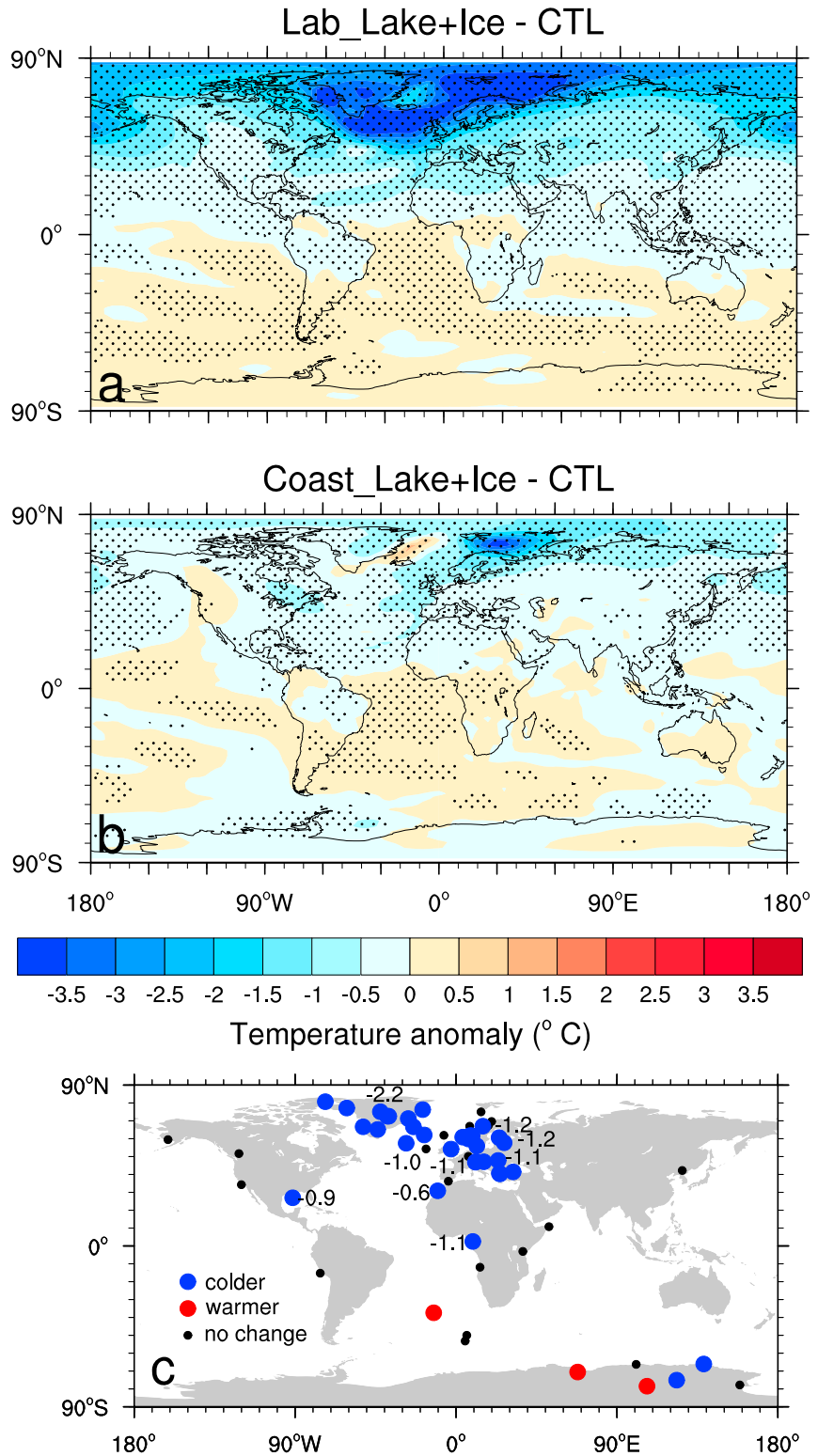


Figure 8. Annual 2 m temperature anomalies for the (a) Lab_Lake + Ice experiment and (b) Coast_Lake + Ice experiment relative to the control, in degrees Celsius, compared with (c) proxy temperature anomalies of the 8.2 ka event relative to early Holocene background climate [Morrill *et al.*, 2013a]. Model anomalies have been calculated for the entire 150 year period of meltwater forcing and recovery. Stippling indicates anomalies that are statistically significant at the 95% level according to a Student's *t* test. Black dots indicate sites with temperature proxies that did not have an identifiable anomaly. Values plotted on the proxy synthesis are quantitative mean annual temperature anomalies in degrees Celsius.

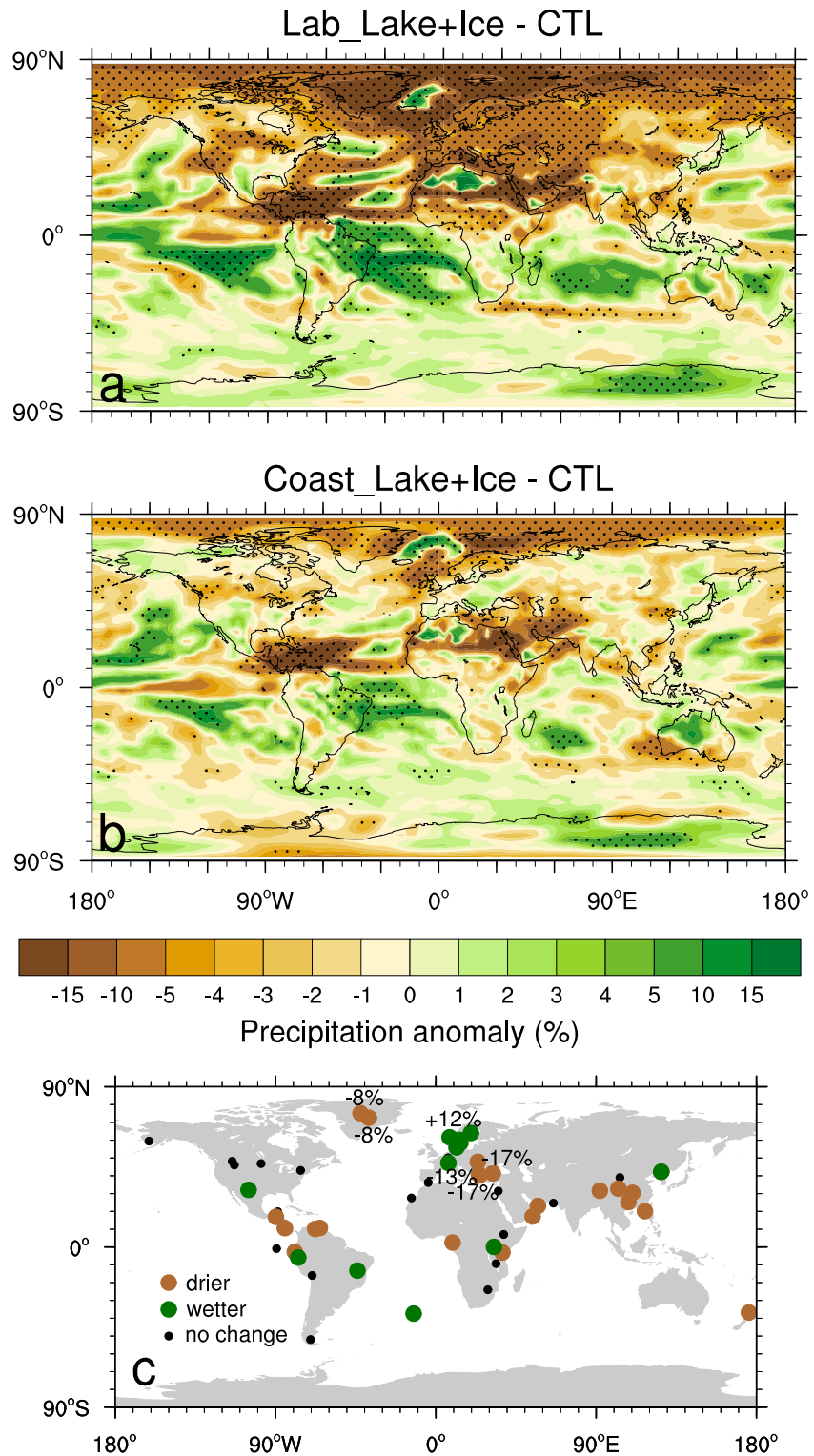
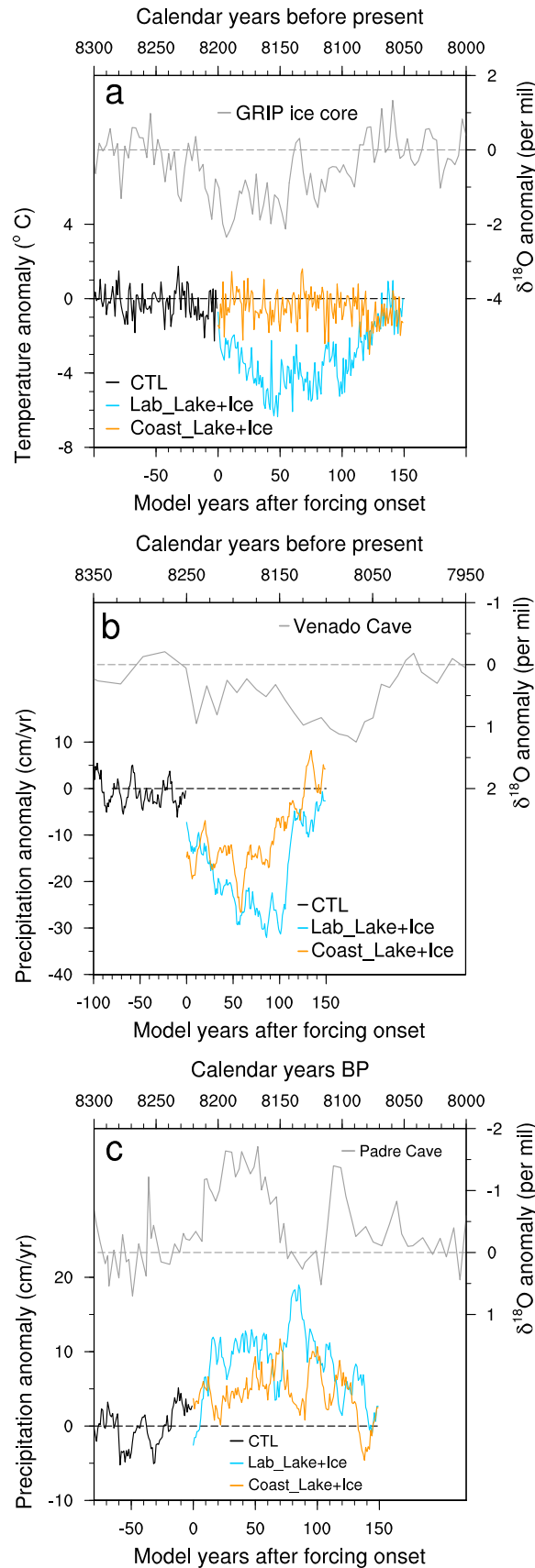


Figure 9. Annual precipitation anomalies for the (a) Lab_Lake + Ice experiment and (b) Coast_Lake + Ice experiment relative to the control, in percent change from the control experiment, compared with (c) proxy precipitation anomalies of the 8.2 ka event relative to early Holocene background climate [Morrill *et al.*, 2013a]. Model anomalies have been calculated for the entire 150 year period of meltwater forcing and recovery. Stippling indicates anomalies that are statistically significant at the 95% level according to a Student's *t* test. Black dots indicate sites with precipitation proxies that did not have an identifiable anomaly. Values plotted on the proxy synthesis are quantitative mean annual precipitation estimates in percent change from early Holocene background climate.



Northward ocean heat transport in the Atlantic decreases in conjunction with the reductions in AMOC (not shown), with percentage declines across simulations similar to those for AMOC. Both the decrease in northward ocean heat transport and the presence of low-salinity ocean surface layers promote sea ice growth in the Northern Hemisphere. The expansion of annual mean Northern Hemisphere sea ice area scales with AMOC and with northward heat transport; sea ice area in Lab_Lake + Ice increases ~16% over the control compared to increases of 3% or less for the other three experiments (Figure 7b).

3.3. Temperature and Precipitation Response

There are also significant differences between the Lab and Coast experiments in the global temperature and precipitation anomalies that result from the meltwater forcing. Given the climate's relatively small and short-lived response in the Lake-only experiments, we discuss only the Lake + Ice experiments here. Annual temperature cools across most of the Northern Hemisphere in both the Lab_Lake + Ice and Coast_Lake + Ice experiments, though the magnitude of cooling is much stronger in Lab_Lake + Ice (Figures 8a and 8b). For example, Northern Hemisphere temperature anomalies are -0.8°C and -0.2°C and circum-North Atlantic ($40^{\circ}\text{--}80^{\circ}\text{N}$, $60^{\circ}\text{W--}30^{\circ}\text{E}$) anomalies are -2.4°C and -0.7°C for the Lab and Coast experiments, respectively, averaged over the 150 years following the onset of meltwater forcing. Both experiments show slight yet statistically significant warming in the Southern Hemisphere, though these anomalies are more spatially extensive in the Lab than in the Coast experiment. Similar to previous

Figure 10. Comparison of proxy $\delta^{18}\text{O}$ time series with output from the Lake + Ice experiments, (a) $\delta^{18}\text{O}$ in per mil SMOW from Greenland Ice Core Project ice core (72.6°N , 37.6°W) [Thomas et al., 2007] and modeled annual 2 m air temperature in degrees Celsius for $70^{\circ}\text{--}80^{\circ}\text{N}$, $35^{\circ}\text{--}55^{\circ}\text{W}$, (b) $\delta^{18}\text{O}$ from Venado Cave in per mil Pee Dee belemnite (PDB) (10.6°N , 84.8°W) [Lachniet et al., 2004] and modeled annual precipitation in cm/yr for $5^{\circ}\text{--}15^{\circ}\text{N}$, $75^{\circ}\text{--}95^{\circ}\text{W}$, and (c) $\delta^{18}\text{O}$ from Padre Cave in per mil PDB (13.2°S , 44.0°W) [Cheng et al., 2009] and modeled annual precipitation in cm/yr for $10^{\circ}\text{--}20^{\circ}\text{S}$, $35^{\circ}\text{--}55^{\circ}\text{W}$. All time series are expressed as anomalies, the proxies from an early Holocene mean and the model experiments from the mean of the control simulation.

experiments [e.g., *Otto-Bliesner and Brady, 2010*], local winter anomalies in each hemisphere are stronger than local summer anomalies largely due to the amplifying effects of winter sea ice cover (not shown).

Likewise, meltwater forcing causes annual precipitation to decline across most of the Northern Hemisphere while increasing across most of the Southern Hemisphere (Figures 9a and 9b). In general, the anomaly patterns observed on the annual basis are also present seasonally (not shown). This pattern is clearer in the extratropics of both hemispheres in the Lab than in the Coast experiment. Interestingly, the signal in the tropics, a southward shift of the Intertropical Convergence Zone (ITCZ), is nearly as large in the Coast experiment as it is in the Lab experiment. For Last Glacial Maximum hosing experiments with the CCSM3, *Otto-Bliesner and Brady [2010]* suggest that southward advection of cold, relatively fresh water in the subtropical gyre reduces atmospheric convection in the Northern Hemisphere tropics and causes the modeled southward shift of the ITCZ. This explanation is also plausible for our results, particularly given that significant southward transport of freshwater in the subtropical gyre occurs in both the Lab and Coast experiments (e.g., Figures 2 and 4). Other proposed causes of a southward shift in the ITCZ include increased sea ice [*Chiang and Bitz, 2005*] and a reduction in the strength of the AMOC [*Chiang et al., 2008*]. Changes in sea ice and AMOC are relatively small in the Coast experiment, however, making it difficult to call upon these mechanisms as an explanation for the large tropical response in this experiment (Figures 9a and 9b).

Overall, the Lab_Lake + Ice experiment matches proxy records of the 8.2 ka event better than the Coast_Lake + Ice experiment does. While both experiments generally capture the spatial patterns of temperature and precipitation change from proxies (Figures 8c and 9c), the magnitude of climate change, particularly for temperature in Greenland and Europe, is better matched by the Lab experiment (Figure 8). Neither of the experiments show the increase in precipitation in northern Europe that is indicated by proxies (Figure 9c), though these proxy records could be more sensitive to snowmelt runoff rather than mean annual precipitation [e.g., *Hammarlund et al., 2005; Hede et al., 2010; Snowball et al., 2010*]. The Lab experiment yields a reasonable match to event duration inferred from proxy records in the circum-North Atlantic region, as demonstrated by an example from Greenland, while anomalies from the Coast experiment are minimal for this region (Figure 10a). For tropical precipitation, however, both experiments match the duration of the 8.2 ka event reasonably well and are successful in simulating reduced precipitation north of the equator and increased precipitation south of the equator (Figures 10b and 10c).

4. Discussion and Conclusions

Our results show that significantly different freshwater transport pathways, as well as ocean and climate responses, result from releasing meltwater just along the Labrador coast as opposed to across all of the Labrador Sea. Meltwater added along the Labrador coast is more likely than freshwater added across the Labrador Sea to be entrained in the subtropical gyre and is less likely to take a northerly path into the Irminger Sea, Iceland Basin, or GIN Seas. The resulting differences in freshwater distribution in the North Atlantic means that AMOC is impacted much less in the Labrador coast experiments than in the Labrador Sea experiments, as is ocean heat transport and extratropical temperature. Interestingly, tropical precipitation patterns are not much affected by the meltwater forcing location for the reasons discussed in section 3.3.

The Lab_Lake + Ice experiment gives the best match to available proxy evidence for ocean salinity anomalies and for both spatial and temporal temperature anomalies (Figures 2, 8, and 10). The change in ocean salinity is too small in the other experiments, particularly in the region of the North Atlantic Current (NAC) south of Iceland. We lack quantitative proxy estimates of the decrease in AMOC at 8.2 ka, but the significant weakening inferred from proxies [e.g., *Ellison et al., 2006; Kleiven et al., 2008*] is probably more in line with the Lab_Lake + Ice result than the much smaller reductions observed in the other experiments. Likewise, circum-North Atlantic temperature anomalies from the Lab_Lake + Ice experiment are the most comparable of the four experiments to quantitative proxy estimates.

The superior match of the Lab_Lake + Ice experiment to proxy evidence is surprising given that physical oceanographic constraints indicate that the meltwater was likely trapped along the Labrador coast and was unlikely to have spread in large volumes across the subpolar gyre into the Labrador Sea [*Wunsch, 2010*], as occurs in the Lab_Lake + Ice experiment. The large amount of freshwater present in the center of the

subpolar gyre in Lab_Lake + Ice is especially troublesome because it causes a large reduction in ocean convection in the Labrador Sea that likely contributes a significant proportion of the deepwater response.

On the other hand, there is proxy evidence that meltwater at 8.2 ka joined the NAC and that significant volumes did reach the Iceland basin and probably the GIN Seas [Came *et al.*, 2007; Ellison *et al.*, 2006; Lewis *et al.*, 2012; Quillmann *et al.*, 2012; Thornalley *et al.*, 2009]. The Lab experiments capture this freshwater distribution better than the Coast experiments do, though perhaps for the wrong reasons. A common model bias, which is present in the CCSM3, is that the Gulf Stream separates from the coast of North America too far north, causing the NAC to follow a path across the North Atlantic that is too zonal compared to observations [Danabasoglu *et al.*, 2014; Large and Danabasoglu, 2006]. This means that the NAC does not spread over the Iceland basin as it should; instead, the Iceland basin is under the influence of the subpolar gyre. In the Lab experiments, the Iceland basin has relatively large freshwater anomalies because the meltwater is added directly into the subpolar gyre and this addition decreases salinity south of Iceland. In the Coast experiments, meltwater largely bypasses the Iceland basin, potentially due to the bias in modeled currents. This model bias could be particularly important for the early Holocene response to meltwater, since it is possible that less deepwater was forming at that time in the Labrador Sea and more was forming in the GIN Seas and the Iceland basin [Hall *et al.*, 2010; Hillaire-Marcel *et al.*, 2001]. In this case, the model bias could prevent the Coast experiments from simulating the correct response, although the possibility that freshwater is routed correctly in the Coast experiments cannot be ruled out until model biases are resolved.

The same model bias in the NAC is shared by the other two high-resolution ocean models to have tested a coastally confined flow at 8.2 ka, the MITgcm [Condrón and Winsor, 2011; Danabasoglu *et al.*, 2014] and the UVic Earth System Model [Spence *et al.*, 2008]. Our results agree with those of Condrón and Winsor [2011] and extend their findings to a fully coupled atmosphere-ocean model that has been run for the entire duration of the 8.2 ka event with the latest meltwater flux estimates. On the other hand, Spence *et al.* [2008] find little sensitivity to the location of freshwater forcing in their model. This result could be caused by additional model biases in convection areas, which are incorrectly located in the eastern Atlantic south of the Iceland-Scotland ridge. Our results also do not agree with those from some other model simulations with lower resolution oceans, in which meltwater additions that are confined to the Labrador coast are spread by ocean currents across the Labrador Sea [LeGrande and Schmidt, 2008; Wiersma *et al.*, 2006]. Condrón and Winsor [2011] suggest that ocean models with these lower resolutions are too diffusive and are therefore unable to maintain meltwater transport that is constrained strictly to the coast and the NAC. Our results do qualitatively agree with the lower resolution simulations of Li *et al.* [2009], however. To simulate a coastally confined flow, these authors add freshwater to several locations along the eastern coast of North America as far south as Cape Hatteras. Freshwater perturbations to these locations cause only minor freshening in the Labrador Sea convection area, resulting in relatively weak and short-lived anomalies compared to freshwater perturbations added nearer to the convection areas.

While they are not as convincing, several other possible explanations exist as to why the more realistic meltwater forcing location (i.e., along the Labrador coast) yields ocean and climate responses that compare poorly to proxy evidence. For example, some amount of the meltwater was likely to have been in the form of icebergs [e.g., Lajeunesse and St-Onge, 2008], and iceberg drift could follow a different path than liquid water since it integrates current directions over the depth of the iceberg. Previous model simulations do not support the argument that a combination of meltwater and icebergs released from the Hudson Strait would have caused a significantly different response than meltwater alone, however, either because the icebergs' path would not have deviated greatly from that of the meltwater [Wiersma and Jongma, 2010] or because icebergs would have taken a more southerly path even further removed from convection areas [Bigg *et al.*, 2011]. Alternatively, either iceberg or meltwater additions to the Arctic Ocean or GIN Seas have been shown to have much larger impacts than the same forcing originating in the Hudson Strait [Bigg *et al.*, 2011; Condrón and Winsor, 2012]. There is good evidence from iceberg scours in the Hudson Bay [Lajeunesse and St-Onge, 2008], as well as from detrital carbonate deposits along the Labrador coast [Lewis *et al.*, 2012], for meltwater at 8.2 ka originating in the Hudson Bay, but there is no additional information either supporting or ruling out other meltwater sources. Lastly, it is possible that the actual freshwater forcing at 8.2 ka was even larger than the volume applied in the Lake + Ice experiments (i.e., greater than 1.35 m of sea level rise) [see, e.g., Hijma and Cohen, 2010]. Given model biases in the NAC, however, a larger forcing might still be mostly routed away from deepwater formation areas.

The CCSM3 experiments presented here likely demonstrate how model biases in ocean circulation are a limitation for correctly simulating the 8.2 ka and other similar events. Given these model biases and the proxy evidence for decreased salinity near North Atlantic convection areas around 8.2 ka, it is premature to conclude that freshwater forcing did not cause the 8.2 ka event [e.g., *Condon and Winsor*, 2011]. Even though experiments such as our Lab experiments, in which meltwater is added to a relatively large area of the ocean, have been criticized as unrealistic [e.g., *Wunsch*, 2010], they still have utility in hindcasting experiments provided that we have proxy evidence supporting the prescribed geographic distribution of freshwater. It is not a perfect approach since it may rely on certain assumptions about the freshwater forcing source and routing, but we often lack other alternatives. Of course, the situation is different for future prediction, which undeniably depends on correctly simulating freshwater transport. Advances are being made in reducing these model biases in ocean circulation [e.g., *Danabasoglu et al.*, 2014], and additional 8.2 ka experiments completed with these improved models will test our interpretations.

Acknowledgments

This research was funded by grants from the National Science Foundation, Office of Polar Programs, to C.M. (ARC-0713951) and B.L.O.-B. (ARC-0713971) and the NOAA Hollings Scholar Program to E.M. W. We thank Anders Carlson for helpful discussions and two anonymous reviewers for substantive comments. Supercomputer time was provided by a grant from the National Center for Atmospheric Research (NCAR) Computational Information Systems Laboratory (CISL). The National Center for Atmospheric Research is sponsored by the National Science Foundation. Model output is available from the corresponding author upon request.

References

- Andersen, C., N. Koç, A. Jennings, and J. T. Andrews (2004a), Nonuniform response of the major surface currents in the Nordic Seas to insolation forcing: Implications for the Holocene climate variability, *Paleoceanography*, *19*, PA2003, doi:10.1029/2002PA000873.
- Andersen, C., N. Koç, and M. Moros (2004b), A highly unstable Holocene climate in the subpolar North Atlantic: Evidence from diatoms, *Quat. Sci. Rev.*, *23*, 2155–2166.
- Barber, D. C., et al. (1999), Forcing of the cold event of 8,200 years ago by catastrophic drainage of Laurentide lakes, *Nature*, *400*, 344–348.
- Berger, A. L. (1978), Long-term variations of caloric insolation resulting from the Earth's orbital elements, *Quat. Res.*, *9*, 139–167.
- Bigg, G. R., R. C. Levine, and C. L. Green (2011), Modelling abrupt glacial North Atlantic freshening: Rates of change and their implications for Heinrich events, *Global Planet. Change*, *79*, 176–192.
- Came, R. E., D. W. Oppo, and J. F. McManus (2007), Amplitude and timing of temperature and salinity variability in the subpolar North Atlantic over the past 10 ky, *Geology*, *35*, 315–318.
- Carlson, A. E., P. U. Clark, B. A. Haley, and G. P. Klinkhammer (2009), Routing of western Canadian Plains runoff during the 8.2 ka cold event, *Geophys. Res. Lett.*, *36*, L14704, doi:10.1029/2009GL038778.
- Cheng, H., D. Fleitmann, R. L. Edwards, X. Wang, F. W. Cruz, A. S. Auler, A. Mangini, Y. Wang, S. J. Burns, and A. Matter (2009), Timing and structure of the 8.2 kyr B.P. event inferred from $\delta^{18}\text{O}$ records of stalagmites from China, Oman, and Brazil, *Geology*, *37*, 1007–1010.
- Chiang, J. C. H., and C. M. Bitz (2005), Influence of high latitude ice cover on the marine Intertropical Convergence Zone, *Clim. Dyn.*, *25*, 477–496.
- Chiang, J. C. H., W. Cheng, and C. M. Bitz (2008), Fast teleconnections to the tropical Atlantic sector from Atlantic thermohaline adjustment, *Geophys. Res. Lett.*, *35*, L07704, doi:10.1029/2008GL033292.
- Clarke, G. K. C., D. W. Leverington, J. T. Teller, and A. S. Dyke (2004), Paleohydraulics of the last outburst flood from glacial Lake Agassiz and the 8200 BP cold event, *Quat. Sci. Rev.*, *23*, 389–407.
- Clarke, G. K. C., A. B. G. Bush, and J. W. M. Bush (2009), Freshwater discharge, sediment transport, and modeled climate impacts of the final drainage of glacial Lake Agassiz, *J. Clim.*, *22*, 2161–2180.
- Cléroux, C., M. Debret, E. Cortijo, J. C. Duplessy, F. Dewilde, J. Reijmer, and N. Massei (2012), High-resolution sea surface reconstructions off Cape Hatteras over the last 10 ka, *Paleoceanography*, *27*, PA1205, doi:10.1029/2011PA002184.
- Collins, W. D., et al. (2006), The Community Climate System Model Version 3 (CCSM3), *J. Clim.*, *19*, 2122–2143.
- Condon, A., and P. Winsor (2011), A subtropical fate awaited freshwater discharged from glacial Lake Agassiz, *Geophys. Res. Lett.*, *38*, L03705, doi:10.1029/2010GL046011.
- Condon, A., and P. Winsor (2012), Meltwater routing and the Younger Dryas, *Proc. Natl. Acad. Sci.*, *109*, 19,928–19,933.
- Danabasoglu, G., et al. (2014), North Atlantic simulations in Coordinated Ocean-ice Reference Experiments phase II (CORE-II). Part I: Mean states, *Ocean Model.*, *73*, 76–107.
- deVernal, A., and C. Hillaire-Marcel (2006), Provincialism in trends and high frequency changes in the northwest North Atlantic during the Holocene, *Global Planet. Change*, *54*, 263–290.
- Dyke, A. S. (2004), An outline of North American deglaciation with emphasis on central and northern Canada, in *Quaternary Glaciations: Extent and Chronology, Part II: North America*, edited by J. Ehlers and P. L. Gibbard, pp. 373–424, Elsevier, Amsterdam, Netherlands.
- Ellison, C. R. W., M. R. Chapman, and I. R. Hall (2006), Surface and deep ocean interactions during the cold climate event 8200 years ago, *Science*, *312*, 1929–1932.
- Farmer, E. J., M. R. Chapman, and J. E. Andrews (2008), Centennial-scale Holocene North Atlantic surface temperatures from Mg/Ca ratios in *Globigerina bulloides*, *Geochem. Geophys. Geosyst.*, *9*, Q12029, doi:10.1029/2008GC002199.
- Flückiger, J., T. Blunier, B. Stauffer, J. Chappellaz, R. Spahni, K. Kawamura, J. Schwander, T. F. Stocker, and D. Dahl-Jensen (2004), N_2O and CH_4 variations during the last glacial epoch: Insight into global processes, *Global Biogeochem. Cycles*, *18*, GB1020, doi:10.1029/2003GB002122.
- Ganachaud, A. (2003), Large-scale mass transports, water mass formation, and diffusivities estimated from World Ocean Circulation Experiment (WOCE) hydrographic data, *J. Geophys. Res.*, *108*(C7), 3213, doi:10.1029/2002JC001565.
- Gregoire, L. J., A. J. Payne, and P. J. Valdes (2012), Deglacial rapid sea level rises caused by ice-sheet saddle collapses, *Nature*, *487*, 219–223.
- Hall, I. R., G. G. Bianchi, and J. R. Evans (2004), Centennial to millennial scale Holocene climate-deep water linkage in the North Atlantic, *Quat. Sci. Rev.*, *23*, 1529–1536.
- Hall, I. R., J. Becker, D. Thornalley, and S. R. Hemming (2010), Holocene variability of North Atlantic deep water: Palaeocurrent reconstruction of component water masses close to their source, in 10th International Conference on Paleoclimatology, La Jolla, Calif.
- Hammarlund, D., S. Björck, B. Buchardt, and C. T. Thomsen (2005), Limnic responses to increased effective humidity during the 8200 cal. yr BP cooling event in southern Sweden, *J. Paleolimnol.*, *34*, 471–480, doi:10.1007/s10933-005-5614-z.
- Hede, M. U., P. Rasmussen, N. Noe-Nygaard, A. L. Clarke, R. D. Vinebrooke, and J. Olsen (2010), Multiproxy evidence for terrestrial and aquatic ecosystem responses during the 8.2 ka cold event as recorded at Højby Sø, Denmark, *Quat. Res.*, *73*, 485–495.
- Hijma, M. P., and K. M. Cohen (2010), Timing and magnitude of the sea-level jump prelude the 8200 yr event, *Geology*, *38*, 275–278.

- Hillaire-Marcel, C., A. de Vernal, G. Bilodeau, and A. J. Weaver (2001), Absence of deep-water formation in the Labrador Sea during the last interglacial period, *Nature*, *410*, 1073–1077.
- Hillaire-Marcel, C., A. de Vernal, and D. J. W. Piper (2007), Lake Agassiz final drainage event in the northwest North Atlantic, *Geophys. Res. Lett.*, *34*, L15601, doi:10.1029/2007GL030396.
- Hoffman, J. S., A. E. Carlson, K. Winsor, G. P. Klinkhammer, A. N. LeGrande, J. T. Andrews, and J. C. Strasser (2012), Linking the 8.2 ka event and its freshwater forcing in the Labrador Sea, *Geophys. Res. Lett.*, *39*, L18703, doi:10.1029/2012GL053047.
- Kendall, R. A., J. X. Mitrovica, G. A. Milne, T. E. Tornqvist, and Y. Li (2008), The sea-level fingerprint of the 8.2 ka climate event, *Geology*, *36*, 423–426.
- Kleiven, H. F., C. Kissel, C. Laj, U. S. Ninnemann, T. O. Richter, and E. Cortijo (2008), Reduced North Atlantic deep water coeval with the glacial Lake Agassiz freshwater outburst, *Science*, *319*, 60–64.
- Lachniet, M. S., Y. Asmerom, S. J. Burns, W. P. Patterson, V. J. Polyak, and G. O. Seltzer (2004), Tropical response to the 8200 yr BP cold event? Speleothem isotopes indicate a weakened early Holocene monsoon in Costa Rica, *Geology*, *32*, 957–960.
- Lajeunesse, P., and G. St-Onge (2008), The subglacial origin of the Lake Agassiz-Ojibway final outburst flood, *Nat. Geosci.*, *1*, 184–188.
- Large, W. G., and G. Danabasoglu (2006), Attribution and impacts of upper-ocean biases in CCSM3, *J. Clim.*, *19*, 2325–2346.
- LeGrande, A. N., and G. A. Schmidt (2008), Ensemble, water isotope-enabled, coupled general circulation modeling insights into the 8.2 ka event, *Paleoceanography*, *23*, PA3207, doi:10.1029/2008PA001610.
- Lewis, C. F. M., A. A. L. Miller, E. Levac, D. J. W. Piper, and G. V. Sonnichsen (2012), Lake Agassiz outburst age and routing by Labrador Current and the 8.2 cal ka cold event, *Quat. Int.*, *260*, 83–97.
- Li, Y.-X., H. Renssen, A. P. Wiersma, and T. E. Tornqvist (2009), Investigating the impact of Lake Agassiz drainage routes on the 8.2 ka cold event with a climate model, *Clim. Past*, *5*, 471–480.
- Li, Y.-X., T. E. Tornqvist, J. M. Nevitt, and B. Kohl (2012), Synchronizing a sea-level jump, final Lake Agassiz drainage, and abrupt cooling 8200 years ago, *Earth Planet. Sci. Lett.*, *315–316*, 41–50.
- Licciardi, J. M., J. T. Teller, and P. U. Clark (1999), Freshwater routing by the Laurentide ice sheet during the last deglaciation, in *Mechanisms of Global Climate Change at Millennial Time Scales*, edited by P. U. Clark, R. S. Webb, and L. D. Keigwin, pp. 177–201, AGU, Washington, D. C.
- Liu, Z., et al. (2009), Transient simulation of last deglaciation with a new mechanism of Bolling-Allerod warming, *Science*, *325*, 310–314.
- Lumpkin, R., and K. Speer (2007), Global ocean meridional overturning, *J. Phys. Oceanogr.*, *37*, 2550–2562.
- McManus, J. F., R. Francois, J.-M. Gherardi, L. D. Keigwin, and S. Brown-Leger (2004), Collapse and rapid resumption of Atlantic meridional circulation linked to deglacial climate changes, *Nature*, *428*, 834–837.
- Monnin, E., A. Indermuhle, A. Dallenbach, J. Fluckinger, B. Stauffer, T. F. Stocker, D. Raynaud, and J.-M. Barnola (2001), Atmospheric CO₂ concentrations over the last glacial termination, *Science*, *291*, 112–114.
- Morrill, C., D. M. Anderson, B. A. Bauer, R. Buckner, E. P. Gille, W. S. Gross, M. Hartman, and A. Shah (2013a), Proxy benchmarks for inter-comparison of 8.2 ka simulations, *Clim. Past*, *9*, 423–432.
- Morrill, C., A. N. LeGrande, H. Renssen, P. Bakker, and B. L. Otto-Bliesner (2013b), Model sensitivity to North Atlantic freshwater forcing at 8.2 ka, *Clim. Past*, *9*, 955–968.
- Oppo, D. W., J. F. McManus, and J. L. Cullen (2003), Deepwater variability in the Holocene epoch, *Nature*, *422*, 277–278.
- Otto-Bliesner, B. L., and E. C. Brady (2010), The sensitivity of the climate response to the magnitude and location of freshwater forcing: Last glacial maximum experiments, *Quat. Sci. Rev.*, *29*, 56–73.
- Otto-Bliesner, B. L., E. C. Brady, G. Clauzet, R. Tomas, S. Levis, and Z. Kothavala (2006), Last Glacial Maximum and Holocene climate in CCSM3, *J. Clim.*, *19*, 2526–2544.
- Otto-Bliesner, B. L., C. D. Hewitt, T. M. Marchitto, E. Brady, A. Abe-Ouchi, M. Crucifix, S. Murakami, and S. L. Weber (2007), Last Glacial Maximum ocean thermohaline circulation: PMIP2 model intercomparisons and data constraints, *Geophys. Res. Lett.*, *34*, L12706, doi:10.1029/2007GL029475.
- Peltier, W. R. (2004), Global glacial isostasy and the surface of the ice-age Earth: The ICE-5G (VM2) model and GRACE, *Ann. Rev. Earth Planet. Sci.*, *32*, 111–149.
- Praetorius, S., J. F. McManus, D. W. Oppo, and W. B. Curry (2008), Episodic reductions in bottom-water currents since the last ice age, *Nat. Geosci.*, *1*, 449–452.
- Quillmann, U., T. M. Marchitto, A. E. Jennings, J. T. Andrews, and B. F. Friestad (2012), Cooling and freshening at 8.2 ka on the NW Iceland Shelf recorded in paired d¹⁸O and Mg/Ca measurements of the benthic foraminifer *Cibicides lobatulus*, *Quatern. Res.*, *78*, 528–539.
- Schmidt, G. A., and A. N. LeGrande (2005), The Goldilocks abrupt climate change event, *Quat. Sci. Rev.*, *24*, 1109–1110.
- Snowball, I., R. Muscheler, L. Zillén, P. Sandgren, T. Stanton, and K. Ljung (2010), Radiocarbon wiggle matching of Swedish lake varves reveals asynchronous climate changes around the 8.2 kyr cold event, *Boreas*, *39*, 720–733, doi:10.1111/j.1502-3885.2010.00167.x.
- Solignac, S., J. Giraudeau, and A. de Vernal (2006), Holocene sea surface conditions in the western North Atlantic: Spatial and temporal heterogeneities, *Paleoceanography*, *21*, PA2004, doi:10.1029/2005PA001175.
- Spence, J. P., M. Eby, and A. J. Weaver (2008), The sensitivity of the Atlantic meridional overturning circulation to freshwater forcing at eddy permitting resolutions, *J. Clim.*, *21*, 2697–2710.
- Thomas, E. R., E. W. Wolff, R. Mulvaney, J. P. Steffensen, S. J. Johnsen, C. Arrowsmith, J. W. C. White, B. Vaughn, and T. Popp (2007), The 8.2 ka event from Greenland ice cores, *Quat. Sci. Rev.*, *26*, 70–81.
- Thornalley, D. J. R., H. Elderfield, and I. N. McCave (2009), Holocene oscillations in temperature and salinity of the surface subpolar North Atlantic, *Nature*, *457*, 711–714.
- Tindall, J. C., and P. J. Valdes (2011), Modeling the 8.2 ka event using a coupled atmosphere-ocean GCM, *Global Planet. Change*, *79*, 312–321.
- Tornqvist, T. E., and M. P. Hijma (2012), Links between early Holocene ice-sheet decay, sea-level rise and abrupt climate change, *Nat. Geosci.*, *5*, 601–606.
- Wagner, A. J., C. Morrill, B. L. Otto-Bliesner, N. Rosenbloom, and K. R. Watkins (2013), Model support for forcing of the 8.2 ka event by meltwater from the Hudson Bay ice dome, *Clim. Dyn.*, *41*, 2855–2873, doi:10.1007/s00382-013-1706-z.
- Wiersma, A. P., and J. I. Jongma (2010), A role for icebergs in the 8.2 ka climate event, *Clim. Dyn.*, *35*, 535–549.
- Wiersma, A. P., H. Renssen, H. Goosse, and T. Fichefet (2006), Evaluation of different freshwater forcing scenarios for the 8.2 ka BP event in a coupled climate model, *Clim. Dyn.*, *27*, 831–849.
- Winsor, K., A. E. Carlson, G. P. Klinkhammer, J. S. Stoner, and R. G. Hatfield (2012), Evolution of the northeast Labrador Sea during the last interglaciation, *Geochem. Geophys. Geosyst.*, *13*, Q11006, doi:10.1029/2012GC004263.
- Wunsch, C. (2010), Towards understanding the Paleocene, *Quat. Sci. Rev.*, *29*, 1960–1967.